PHYSICAL REVIEW B **81**, 020505(R) (2010)

Transport phase diagram for superconducting thin films of tantalum with homogeneous disorder

Yize Li,[1] Carlos L. Vicente,[1,2] and Jongsoo Yoon[1]
[1]*Department of Physics, University of Virginia, Charlottesville, Virginia 22904, USA*
[2]*Universidad Puerto Rico, San Juan 00931, Puerto Rico*

(Received 9 October 2009; revised manuscript received 2 December 2009; published 14 January 2010)

We have constructed a phase diagram in temperature–magnetic-field–disorder space for homogeneously disordered superconducting Ta thin films. We identify the phases by measuring nonlinear transport characteristics that are known to be unique in each phase. The resulting phase diagram shows that the superconducting phase is completely surrounded by the intervening metallic phase prohibiting a direct superconductor-insulator transition at any disorder.

DOI: 10.1103/PhysRevB.81.020505 PACS number(s): 74.70.Ad, 74.40.−n

In two dimensions, a true superconducting state with zero electrical resistance is believed to exist only at zero temperature ($T=0$). Increasing disorder or applying magnetic fields (B) can disrupt the superconductivity rendering the system to an insulating state.[1–13] The transition between these two states in disordered films, however, is shrouded in mystery. While conventional theories[2–5] expect a direct superconductor-to-insulator transition (SIT), a mysterious metallic phase intervening the two phases has been observed in several material systems.[6–13] The metallic phase is usually identified by a drop in resistance followed by saturation to a finite value as $T\rightarrow 0$, distinguishable from the superconducting phase where the resistance becomes "immeasurably" small, and the insulating phase where the temperature coefficient of resistivity ($d\rho/dT$) is negative. Such a metallic behavior is particularly pronounced in Ta,[8–10] MoGe,[11,12] and NbSi[13] films, suggesting that it might correspond to a new phase of matter. Three competing paradigms have been proposed to account for the emergence of the metallic phase. The quantum vortex picture[14] describes the metallic phase as a Fermi liquid of interacting vortices (vortex metal), the percolation paradigm[15–18] describes the films as consisting of superconducting and normal puddles, and the phase glass model[19,20] attributes the metallic transport to the coupling of the bosonic degrees of freedom to the excitations of the glassy phase.

So far, most of the experimental studies on the unexpected metallic phase are carried out in the lowest accessible T. This is in part because the studies are more focused on the $T=0$ ground state, and in part because of the lack of established experimental probes to characterize the metallic transport at elevated T. Recently, however, systematic studies on Ta films have shown that each phase exhibits distinctly different nonlinear transport properties, providing alternative criteria to identify phases as described below.[9] While the phase identification by the nonlinear transport is fully consistent with that based on the T dependence of ρ, it also allows us to unambiguously identify phases at any point in the T-B plane. In this Rapid Communication, we present a three-dimensional (3D) phase diagram in T-B-disorder space derived from nonlinear transport measurements on Ta films with different thicknesses representing different degrees of disorder. The phase diagram shows that the superconducting phase is completely surrounded by the metallic phase prohibiting a direct SIT at any disorder.

We first discuss the rationale behind the nonlinear transport-based phase identification. The superconducting phase is unique in displaying hysteresis in the current-voltage (I-V) curve. As shown in Fig. 1(b) for $B\leq 0.12$ T, with increasing current (I) the superconducting state is abruptly quenched at a well-defined critical current, which corresponds to an electronic instability. It is known that such an instability can arise from a Joule heating which can cause a thermal runaway to the normal conducting state.[21] In this heating scenario, the critical power, $P_c=I_cV_c$, where I_c and V_c are the current and voltage at the instability along the I-increasing branch, is expected to be a weakly decreasing function of B.[21] However, P_c is found to increase exponentially by an order of magnitude by applying B of magnitude less than a few gauss, demonstrating that the instability has a nonthermal origin.[8] The important observations are that with

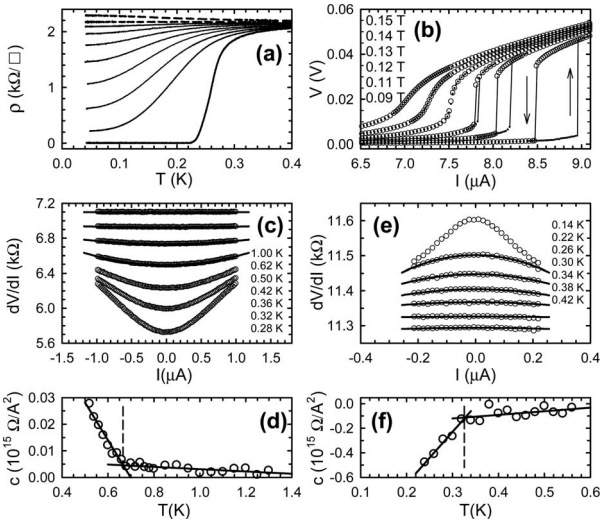

FIG. 1. (a) Sheet resistance vs T for Ta 2 at various B in the range 0–0.5 T. (b) I-V curves of Ta 1 at $T=0.1$ K at the indicated B. Filled (open) circles are for current increasing (decreasing) branch. The solid lines are to indicate the electronic instabilities, and the arrows show the direction of the change. (c) dV/dI vs I of Ta 1 at $B=0.6$ T at the indicated T. The solid lines are the fit to the quadratic function. (d) The quadratic coefficients from the fitting are plotted for Ta 1. The solid lines are a guide to the eye, and the dashed line corresponds to the metal-normal conductor phase boundary. (e) dV/dI vs I for Ta 2 at $B=2.0$ T at the indicated T. Solid lines are fit to the quadratic function. (f) Quadratic coefficients vs T for sample Ta 2. The dashed line corresponds to the insulator-normal conductor boundary.

TABLE I. List of sample parameters: nominal film thickness t, normal-state sheet resistance ρ_n at 4.2 K, and the observed phases in each sample (S for superconducting phase, M for the metallic phase, I for the insulating phase, and N for the normal conducting phase). For samples exhibiting the superconducting phase, we list mean field T_c at $B=0$, the critical magnetic field B_c as defined by the field at which the resistance reaches 90% of the high-field saturation value, and the correlation length calculated from $\xi=\sqrt{\Phi_0/2\pi B_c}$, where Φ_0 is the flux quantum.

Films	Batch	t (nm)	ρ_n (k$\Omega/\square$)	Phase	T_c (K)	B_c (T)	ξ (nm)
Ta 1	1	5.6	1.42	S,M,I,N	0.65	0.82	20
Ta 2	2	4.1	2.28	S,M,I,N	0.26	0.33	32
Ta 3	3	2.5	3.04	M,I,N			
Ta 4	3	2.4	3.34	M,I,N			
Ta 5	3	2.3	3.54	M,I,N			
Ta 6	3	2.2	3.88	M,I,N			
Ta 7	3	2.1	4.20	I,N			
Ta 8	3	2.0	4.98	I,N			
Ta 9	3	1.0	6.20	I,N			
Ta 10	4	2.5	6.24	I,N			
Ta 11	5	2.5	8.00	I,N			

approaching the instability the electronic relaxation-time constant becomes increasingly longer, reaching up to several seconds, and that the instabilities of the same characteristics are observed on films with normal-state resistivity (ρ_n) much less than 100 $\Omega/\square$. These observations are consistent with the picture that the instabilities correspond to the vortex pinning-depinning phenomena arising from the competition between Lorentz driving force on the vortices and the disorder-induced pinning force.[22] In this picture, all the vortices are expected to be pinned at $T=0$ implying a realization of zero resistance state, and thus the superconducting phase.

As the system is driven into the metallic phase with increasing B, the hysteresis in the superconducting phase becomes progressively smaller and evolves into the point of the largest slope in the continuous and reversible I-V as shown in Fig. 1(b). This demonstrates that the hysteresis in the superconducting phase and the metallic nonlinear transport characterized by $d^2V/dI^2>0$ are caused by the same mechanism. Furthermore, the metallic nonlinear transport accompanies an electronic relaxation-time constant as long as several seconds, attesting that the transport involves unusual electronic processes.[8] Within the vortex dynamics picture, while in the superconducting phase most of the vortices catastrophically depin at a critical current, in the metallic phase the depinning process occurs gradually leading to the characteristic nonlinear transport. In this picture, the metallic phase corresponds to the regime where pinned and depinned vortices coexist even at zero-bias current resulting in a finite resistance at $T=0$. The insulating phase can be identified by the nonlinear transport with $d^2V/dI^2<0$. Although the origin of the insulating nonlinear transport is not known, we take it as a phenomenological indicator to distinguish the phase.

The results reported in this Rapid Communication are from Ta films with ρ_n ranging 0.07–700 k$\Omega/\square$. Parameters of 11 samples whose data are shown in this Rapid Communication are summarized in Table I. Ta films are dc sputter deposited on Si substrate and patterned into a Hall bar geometry (1×5 mm^2) for four-point measurements using a shadow mask. Ta films are structurally amorphous and homogeneously disordered as reported elsewhere.[9] Special care was taken to avoid noise by using inline filters and performing the measurements inside an electromagnetically shielded room. The T dependence of ρ was measured with 1 nA dc current over a period of $\sim$10 h per trace. Nonlinear transport (I-V curves and dV/dI traces) was measured at a constant bias current that was changed in small discrete steps. dV/dI was measured with a lock-in by modulating the dc bias current with a small amplitude at $\sim$7 Hz, and the results were cross checked by the numerically obtained dV/dI's from dc I-V curves. Near the superconductor-metal (S-M) boundary, dV/dI measurements were not practical because of the long electronic relaxation time. The S-M boundary was mapped by measuring dc I-V curves where we recorded the voltage responses after steady states were reached.

The S-M boundary is determined as T or B at which the hysteresis in I-V first disappears. An example is shown in Fig. 1(b). With increasing B the hysteresis first disappears at $B\approx0.13$ T, which we identify as the S-M boundary.

As shown in Fig. 1(c), the nonlinearity progressively becomes weaker with increasing T and eventually the transport becomes linear. The linear transport at high T is natural because at sufficiently high T the system must become a normal conductor with a linear transport. In order to quantitatively identify the phase boundary, we fit the dV/dI vs I trace to a quadratic function $dV/dI=cI^2+\rho_0$, where c is the quadratic coefficient and ρ_0 is the sample's resistance at $I\rightarrow0$. When the nonlinearity is relatively weak, the fitting is reasonable (the solid curves for the top four traces). In Fig. 1(d) the quadratic coefficients are plotted as a function of T. The behavior of the quadratic coefficients changes abruptly at a well-defined T marked by a dashed line. At low T the coef-

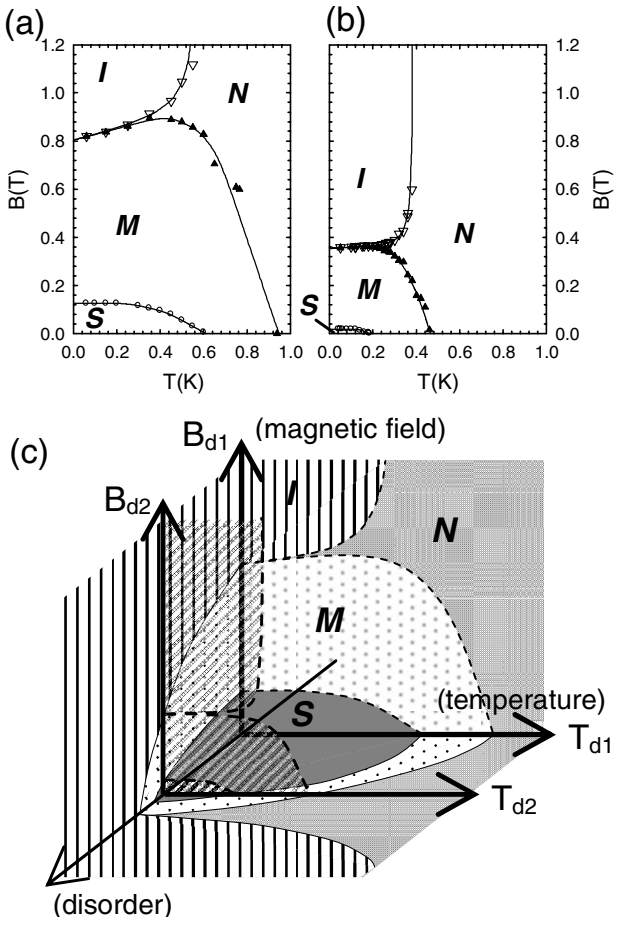

FIG. 2. (a) Phase diagram of Ta 1 in the B-T plane. Symbols are experimental data and solid lines are to guide the eye. The superconducting phase is marked by S, the metallic phase by M, the insulating phase by I, and the normal conducting phase by N. (b) Phase diagram of Ta 2. (c) The topology of the 3D phase diagram in T-B-disorder space is shown. Disorder is represented by ρ_n and the disorder axis indicates only the direction of increasing disorder. The illustrated phase diagram does not include the clean limit.

ficients are rather strongly T dependent. At high T they are almost T independent and the values are close to zero implying a linear transport. We identify the dashed line as the phase boundary separating the metallic phase and the normal conducting phase.

Figure 1(e) shows a similar evolution of the nonlinear transport in the insulating phase. When the nonlinearity is relatively weak the quadratic fitting is reasonable [solid lines in Fig. 1(e)]. Again, as shown in Fig. 1(f), there is a well-defined T across which the behavior of the quadratic coefficients is distinctly different. We identify the low-T regime (below the dashed line) as the insulating phase, and the high-T regime where the coefficients are almost T independent and almost zero as the normal conducting phase.

The phase boundaries determined as described above are shown in Figs. 2(a) and 2(b) for two samples, Ta 1 and Ta 2. Both samples are relatively weakly disordered and all four phases appear. The superconducting phase is marked by S, the metallic phase by M, the insulating phase by I, and the high-T normal conducting phase by N. As represented by their ρ_n Ta 2 is more disordered than Ta 1. The results from

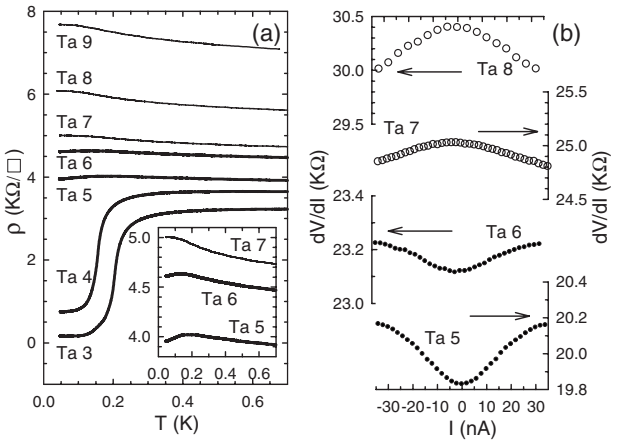

FIG. 3. (a) T dependence of ρ for samples Ta 3–9 at $B=0$ is shown. All these samples are grown in a single batch. (Inset) A blowup view of resistance behavior at low T for samples Ta 5–7. (b) dV/dI vs I for samples Ta 5–8. The arrows indicate the corresponding scale for each trace.

these two samples capture the main feature that both the superconducting and the metallic phases shrink to lower-T and lower-B region with increasing disorder and the insulating phase extends to lower B. This tendency is depicted in the 3D phase diagram in the T-B-disorder space in Fig. 2(c), where the phase diagram of Ta 1 (Ta 2) corresponds to a cross-sectional view in the T_{d1}-B_{d1} (T_{d2}-B_{d2}) plane.

With further increasing disorder, we reach the regime where the superconducting phase no longer exists even at $T=0$ and $B=0$. This regime appears as a gap between the superconducting and insulating phases along the disorder axis in Fig. 2(c) occupied by the metallic phase. Examples of the metallic behavior at $B=0$ is shown in Fig. 3(a) as thick solid lines. The bottom two traces exhibit a steep drop in ρ followed by saturation to a finite value as $T\rightarrow 0$. Samples Ta 5 and Ta 6 show only a weak T dependence. However, as shown in the inset their slopes are positive at low T and their nonlinear transport is characterized by $d^2V/dI^2>0$ [filled circles in Fig. 3(b)]. We emphasize that these disorder-induced metallic behaviors at $B=0$ are indistinguishable from the B-induced metallic behaviors of samples of weaker disorder such as Ta 1 or Ta 2. For even more disordered samples (samples Ta 7–9), $d\rho/dT$ is always negative with nonlinear transport of $d^2V/dI^2<0$ [open circles in Fig. 3(b)], which are the insulating characteristics. In this high disorder regime where only the insulating phase appears at low T, the boundary of the insulating phase grows to a higher T with increasing disorder. This tendency is shown in Figs. 4(a)–4(c).

With the disorder-induced metallic phase at $B=0$ the superconducting phase is completely surrounded by the metallic phase prohibiting a direct SIT at any disorder. This is a fundamental difference from the phase diagram proposed earlier.[23] Authors of Ref. 23, based on their scaling analysis, have proposed a phase diagram where the metallic phase can exist only in weak disorder regime under finite B. In their phase diagram, a direct SIT occurs in a relatively high disorder regime. While this discrepancy between the two phase diagrams is a puzzle, we note that all the samples interpreted

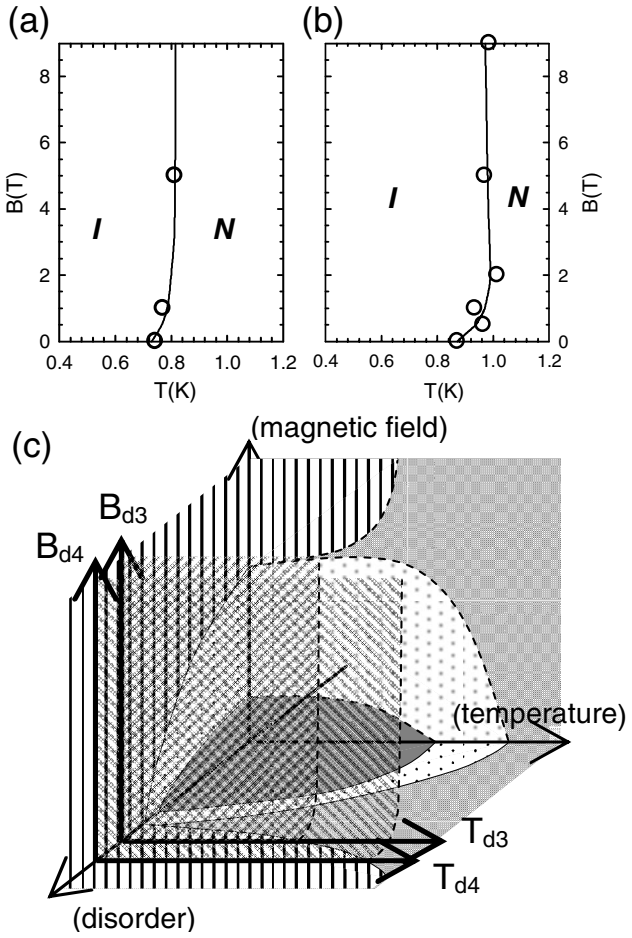

FIG. 4. (a) Phase diagram of Ta 10 in the T-B plane. Insulating phase is marked by I and the normal conducting phase by N. Solid lines are to guide the eye. (b) Phase diagram of Ta 11, which is more disordered than Ta 10 by the measure of ρ_n. (c) The same 3D phase diagram shown in Fig. 2(c), but includes the corresponding cross-sectional views for Ta 10 (T_{d3}-B_{d3} plane) and Ta 11 (T_{d4}-B_{d4} plane).

to exhibit a direct SIT in Ref. 23 are InO material systems which are known to have a wide resistive superconducting transition. Typically, the width of the transition in InO ($\Delta T_c/T_c$), with ΔT_c being the T interval corresponding to the resistance change from 90% to 10% of ρ_n, is larger than that observed in Ta systems by several times or more. $\Delta T_c/T_c$ can be a measure of disorder at a length scale longer than the superconducting coherence length. However, what role this long length scale disorder plays is not clear at present.

Finally, we turn to the discussion on the metallic phase appearing in the $B=0$ finite T region. One might argue that the nonlinear transport of $d^2V/dI^2>0$ could come from the Kosterlitz-Thouless (KT) mechanism.[24] The KT theory has been the framework to understand the two-dimensional superconductivity at a finite T, and it describes the superconducting transition as a thermodynamic instability of vortex-antivortex pairs. The transport in the superconducting phase is expected to follow a power law, $V \propto I^{\alpha}$ (with $\alpha>3$), due to the current-induced vortex pair dissociations.[25] It has been argued[26] that a finite-size effect can induce free vortices altering the power law. The resulting nonlinear transport obtained in a numerical simulation[26] closely resembles what is observed in our samples. However, there are two transport properties that cannot be reconciled with the KT picture: one is the extraordinarily long relaxation time, up to several seconds, and the other is the development of electronic instabilities at low T.[8,9] These observations indicate that the metallic nonlinear transport in the $B=0$ finite T region is unlikely related to the KT mechanism and raise the possibility that the KT transition might have been pre-emptied by a first-order vortex pinning-depinning transition.

In summary, we have mapped a phase diagram in T-B-disorder space for homogeneously disordered superconducting Ta films: the superconducting phase is identified by the presence of electronic instability possibly due to vortex pinning-depinning mechanism, the metallic phase by $d^2V/dI^2>0$, the insulating phase by $d^2V/dI^2<0$, and the normal conducting phase by $d^2V/dI^2=0$. The resulting phase diagram shows that the superconducting phase is completely surrounded by the intervening metallic phase prohibiting a direct SIT at any disorder, and that the metallic phase extends to $B=0$ finite T region.

The authors acknowledge fruitful discussions with G. Refael and H. Fertig. This work was supported by the NSF through Grant No. DMR-0239450.

[1] A. M. Goldman and N. Markovic, Phys. Today **51**(11), 39 (1998).
[2] A. Finkelshtein, JETP Lett. **45**, 46 (1987).
[3] A. Larkin, Ann. Phys. (Leipzig) **8**, 785 (1999).
[4] M. P. A. Fisher, Phys. Rev. Lett. **65**, 923 (1990).
[5] M. P. A. Fisher *et al.*, Phys. Rev. Lett. **64**, 587 (1990).
[6] S.-Y. Hsu *et al.*, Phys. Rev. Lett. **75**, 132 (1995).
[7] J. S. Parker *et al.*, EPL **75**, 950 (2006).
[8] Y. Seo *et al.*, Phys. Rev. Lett. **97**, 057005 (2006).
[9] Y. Qin *et al.*, Phys. Rev. B **73**, 100505(R) (2006).
[10] C. L. Vicente *et al.*, Phys. Rev. B **74**, 100507(R) (2006).
[11] N. Mason and A. Kapitulnik, Phys. Rev. B **65**, 220505(R) (2002).
[12] D. Ephron *et al.*, Phys. Rev. Lett. **76**, 1529 (1996).
[13] H. Aubin *et al.*, Phys. Rev. B **73**, 094521 (2006).
[14] V. M. Galitski *et al.*, Phys. Rev. Lett. **95**, 077002 (2005).
[15] E. Shimshoni *et al.*, Phys. Rev. Lett. **80**, 3352 (1998).
[16] A. Ghosal *et al.*, Phys. Rev. B **65**, 014501 (2001).
[17] Y. Dubi *et al.*, Phys. Rev. B **73**, 054509 (2006).
[18] B. Spivak *et al.*, Phys. Rev. B **77**, 214523 (2008).
[19] D. Dalidovich and P. Phillips, Phys. Rev. Lett. **89**, 027001 (2002).
[20] J. Wu and P. Phillips, Phys. Rev. B **73**, 214507 (2006).
[21] A. V. Gurevich and R. G. Mints, Rev. Mod. Phys. **59**, 941 (1987), and references therein.
[22] Y. Paltiel *et al.*, Phys. Rev. B **66**, 060503(R) (2002).
[23] M. A. Steiner *et al.*, Phys. Rev. B **77**, 212501 (2008).
[24] J. D. Kosterlitz and D. J. Thouless, J. Phys. C **6**, 1181 (1973).
[25] B. I. Halperin *et al.*, J. Low Temp. Phys. **36**, 599 (1979).
[26] K. Medvedyeva *et al.*, Phys. Rev. B **62**, 14531 (2000).